https://doi.org/10.5194/tc-2022-179
Preprint. Discussion started: 30 September 2022

The Cryosphere
Discussions
Open Access

Comprehensive evaluation of black carbon effect on glacier melting on the Laohugou Glacier No. 12, Western Qilian Mountains

Jizu Chen[1], Wentao Du[1*], Shichang Kang[1,4], Xiang Qin[1], Weijun Sun[2], Yang Li[5], Yushuo Liu[1], Lihui Luo[6], Youyan Jiang[3]

[1] Qilian Shan Station of Glaciology and Eco-environment, State Key Laboratory of Cryospheric Science, Northwest Institute of Eco-Environment and Resources, Chinese Academy of Sciences (CAS), Lanzhou 730000, China;

[2] College of Geography and Environment, Shandong Normal University, Jinan 250014, China;

[3] Lanzhou regional climate center, Lanzhou 730020, China;

[4] College of Resources and Environment, University of Chinese Academy of Sciences (UCAS), Beijing 100049, China;

[5] Institute of International Rivers and Eco-security, Yunnan University, Kunming, Yunnan, 650500, China

[6] Northwest Institute of Eco-Environment and Resources, Chinese Academy of Science (CAS), Lanzhou 730000, China;

*Corresponding author address: Name: Wentao Du; E-mail: duwentao@lzb.ac.cn

Abstract:

Global warming and surface albedo reduction by black carbon (BC) in glacier jointly accelerated glacier melting, but their respective contributions remain unclear. This study developed a dynamic deposition model of light absorbing particles (LAPs), which coupled with a surface energy and mass balance model. Based on the coupled model, we further assessed atmospheric deposited BC effect on glacier melting for a period of September 2011 – August 2012 on the Laohugou glacier No. 12 in the western Qilian Mountains. It was found that BC in glacier surface caused 13.1% of annual glacier-wide melting, of which atmospheric direct deposited BC reduced albedo with 0.02 and accounted for 9.1% of glacier melting. The air temperature during recent two decades has increased by 1.5 °C relative to that during 1950s, which accounted for 51.9% of current glacier melt. Meanwhile, based on the BC emission increased by 4.6 times compared to the early Industrial Evolution recorded in an ice core, the increased BC accounted conservatively for 6.7% of current glacier melting. Despite the importance of LAPs regarding glacier melting, their variation on the ice surface remains unclear, and relevant observations are urgently needed to improve simulation of the process.

Keywords: Glacier melting; Black carbon; Simulation; Laohugou Glacier No. 12

https://doi.org/10.5194/tc-2022-179
Preprint. Discussion started: 30 September 2022

The Cryosphere Discussions Open Access EGU

1 Introduction

Light absorbing particles (LAPs), consisting primarily of mineral dust (MD) and black carbon (BC), strongly absorb solar radiation, reduce surface albedo, and intensify glacier melting (Bond et al., 2013; Zhang et al., 2018; Qian et al., 2015). The major sources of BC are human activities related to combustion of fossil and solid fuels, burning of biomass for domestic purposes, while the minor sources are predominantly natural, such as forest fires and volcanic eruptions (Bond et al., 2013). Considering the close link between human activities and BC, a number of studies have investigated the impact of BC on glacier melting (Kang et al., 2020; Ming et al., 2008; Xu et al., 2009; Kaspari et al., 2015).

Over the past 100 years, High Mountains Asia glaciers have generally been retreating slowly (Azam et al., 2018; Yao et al., 2012; Farinotti et al., 2019), but their rates of melting and retreat have been accelerating since the 1990s (Maurer et al., 2019; Brun et al., 2017; Hugonnet et al., 2021; Li et al., 2011). Rapid rise in the global temperature is regarded as the major cause of the accelerating glacier melting since the 1990s; however, the amount of deposited atmospheric BC in northwest of China has also increased dramatically (Wang et al., 2015; Han et al., 2015). Many studies have simulated glacier melting using the temperature index method (Liu et al., 2009; Hock, 2003; Zhang et al., 2006), owing to its applicability and availability of input data. the melting index is a mathematical expression that reflects glacier surface conditions and the state of the atmosphere, and BC is one of the variables that affect the melting index. Given the synchronous increases in global temperature and BC emission, it is important to ascertain the contribution of each to the current accelerated glacier melting.

Previous related research on glacier melting generally focused on assessing the impact attributable to the total amount of BC in surface snow and ice, rather than that attributable to simultaneous direct deposited atmospheric BC (Li et al., 2016; Li et al., 2019c; Li et al., 2019a; Zhang et al., 2017a), this part of BC was directly associated with current human activities and policymaking. However, results obtained through analysis of snow and ice samples using the conventional Environics method, are

https://doi.org/10.5194/tc-2022-179
Preprint. Discussion started: 30 September 2022

transient and discrete with high uncertainty, and it is not possible to separate the BC associated with current human activities from the total historical accumulated BC content in a snow and ice sample. Therefore, we developed a parameterization of a process-based simulation of LAPs deposition, which we coupled with a surface energy and mass balance model. The model was applied to Laohugou Glacier No. 12 (LHG glacier) in the western Qilian Mountains to assess the effect of atmospheric deposition of BC on the current accelerated glacier melting. The purpose of this research is to reveal potential contribution of atmospheric deposited BC to glacier melting in the context of current human emissions, rather than accurate value of it on a certain year. Therefore, we collected BC measurements in snow, ice and atmosphere as complete as possible, though those measurements collected in different year.

2 Study Site and Data

The LHG glacier (39°26.4’N, 96°32.5’E) is the biggest valley-type glacier with an area of 21.08 km^2 in the western Qilian Mountains in the northeast of the Tibetan Plateau. The glacier descends over the range of elevation from 5481 to 4260 m a.s.l. (Fig. 1). Mean annual equilibrium line altitude (ELA) was 5050 m, and annual glacier mass balance was − 213 mm w.e. during 2010–2012 (Chen et al., 2017). An automatic weather station (AWS), installed in 2009 at the site of confluence of two branches, records meteorological variables of air temperature, relative humidity, wind speed, incoming shortwave and longwave radiation, outgoing shortwave and longwave radiation, precipitation. Full details of the AWS and rain gauge instruments can be found in Chen et al. 2018 Data from the AWS acquired between September 2011 and August 2012 was used to initiate the surface energy and mass balance model. Data quality was strictly controlled through test of threshold and extreme value and through ensuring consistency of meteorological variables. Moreover, erroneous data were manually checked, validated, and either corrected or removed.

A snow pit (depth: 105 cm) was dug in the accumulation zone (5040 m a.s.l) of LHG glacier in 2016, and the BC concentration was measured at 5 cm intervals (Fig. 2a), the analyses could be seen in Li et al. 2019c. Additionally, an ice pit was also dug in 2016

https://doi.org/10.5194/tc-2022-179
Preprint. Discussion started: 30 September 2022

(Li et al., 2019b), and its surface and interior concentrations were used as initial conditions for the model (Table 1). Daily BC concentration in the atmosphere was measured using an AE-31 aethalometer built at a natural moraine platform approximately 2 km from the glacier terminal (Fig. 1), the data acquisition spanned from May 2009 to March 2010 (Zhao et al., 2012). The monthly variation of atmospheric BC concentration is shown in Fig. 2b.

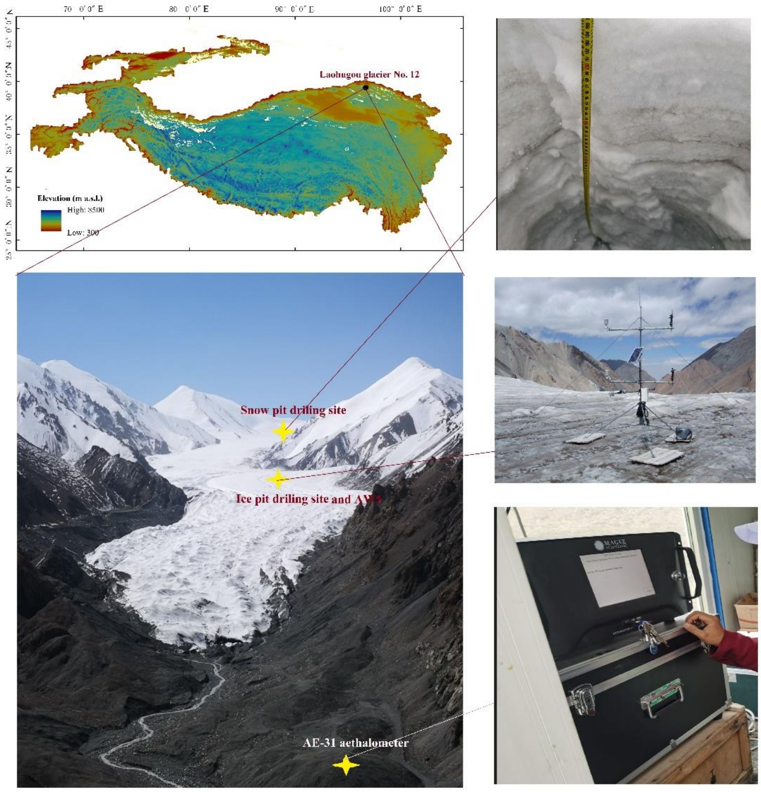

Fig.1 Location map of Laohugou Glacier No. 12 and the distribution of sites for collecting samples of light-absorbing particles.

3 Methods

3.1 Model of atmospheric dry and wet deposition of LAPs

We used the BC concentration in fresh snow on the LHG glacier in 2016 (Li et al., 2019c) as reference for the BC concentration in precipitation. The content of BC deposited by a precipitation event was obtained by multiplying the BC concentration in

https://doi.org/10.5194/tc-2022-179
Preprint. Discussion started: 30 September 2022

precipitation by the precipitation amount. In the case of atmospheric dry deposition of BC, we assumed that adding the BC lost in melted snow to the total content of BC in the snow pit reflected the total content of BC deposited by the atmosphere in a year. Thus, subtracting the BC content of precipitation from the total content of BC provided the total content of atmospheric dry deposition of BC in a year. The monthly deposition rate was obtained according to the total content of atmospheric dry deposition and distribution of monthly atmospheric BC concentration. The same overall method was adopted for the deposition rate of MD; however, the only difference was that MD would not be removed by meltwater owing to its larger particle size (Gabbi et al., 2015; Dong et al., 2014).

At the depth of 65–70 cm in the snow pit, an extremely dirty layer with the highest concentration of BC (1746 ng g^{-1}) indicated that the layer was formed by the intense melting at the end of summer in 2015. Therefore, the snow pack above this layer accumulated during the hydrological year of 2015/2016. The total accumulated BC in the snow pit (5763 ng cm^{-2}) was determined according to the BC concentration and density of each snow layer. The total measured amount of precipitation between September 2015 and August 2016 was 502 mm w.e.; therefore, according to the BC concentration in precipitation, the amount of BC accumulated from precipitation was 1094 ng cm^{-2}. The amount of BC lost in melting snow was obtained by first subtracting the accumulation of snow from the total precipitation. Then, the content of lost BC (786 ng cm^{-2}) was determined according to the amount of melted snow, average BC concentration, and the removal efficiency. Finally, we obtained the total dry deposited BC content (7204 ng cm^{-1}) in terms of the total amounts of BC in the snow pit, precipitation, and loss in meltwater. During the model run, we assigned the dry deposited BC content to the surface at the end of each day according to the distribution of the monthly variation of atmospheric BC concentration. The right-hand ordinate axis in Figure S1b represents the computed range of the daily deposition rate, with values spanning from 8.3 ng d^{-1} cm^{-2} in November to 30.3 ng d^{-1} cm^{-2} in July (Fig. 2b).

https://doi.org/10.5194/tc-2022-179
Preprint. Discussion started: 30 September 2022

The Cryosphere Discussions
Open Access
EGU

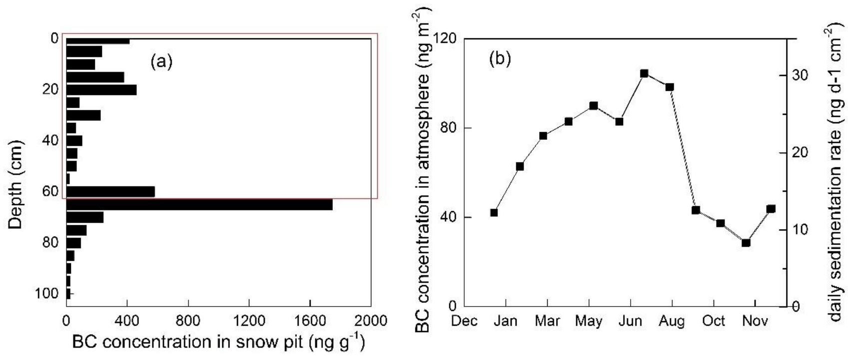

Fig. 2 (a) BC concentration at 5 cm intervals in the snow pit (red frame shows the snow layers accumulated during September 2015 to August 2016). (b) Distribution of monthly BC concentration in the atmosphere (left) and daily sedimentation rate (right).

3.2 Snow layer and impurity model

We divided the entire snow pack into three layers: top 2 cm, middle layer represented by recent snowfall, and rest of snow pack. The thickness, concentration of LAPs (BC and MD), specific surface area (SSA), and water content of each snow layer were recorded by the model. In the case of snowfall greater than 2 cm, the first 2 cm of fresh snow was set as the top layer, the remainder of the fresh snow was set as the middle layer, and the old snow pack was set as the rest of the snow pack layer. All snow parameters were recalculated homogeneously according to the thickness, concentration, and water content of each old layer. In the case of snowfall of less than 2 cm, the top layer was mixed uniformly with the fresh snow.

The middle snow layer was depleted by ablation. If the second snow layer disappeared completely, then the snow in the third layer began to become depleted. To avoid increasing the concentration of LAPs infinitely, the LAPs in the snow layer were gradually mixed with LAPs in the ice surface when the depth of the entire snow layer was less than 2 cm. Water content was calculated by the model; if the water content reached the maximum value, any remaining water percolated into the next layer below. The LAPs contained in evaporated or sublimated snow were all enriched in the surface, whereas a proportion of the LAPs contained in meltwater was removed with the meltwater, while the remainder was enriched in the surface. According to previous

https://doi.org/10.5194/tc-2022-179
Preprint. Discussion started: 30 September 2022

studies, larger particles (>5 μm) generally remain in the snow (Conway et al., 1996), whereas smaller snow impurities (~0.2 μm) are washed out by approximately 10%–30% per mass of melt(Doherty et al., 2013). The observed diameter of BC mass was centered on 0.18 μm in summer and on 0.22 μm in winter (Zhang et al., 2017b); thus, we adopted a removal efficiency of 20% for BC, as suggested both by Gabbi et al. 2015 and by Flanner et al. 2007. Given the larger size of MD on the LHG glacier (Dong et al., 2014), we assumed that MD was unaffected by wash-out of meltwater.

When glacier ice was exposed, we considered the meltout of englacial LAPs, except in the case of atmospheric deposition (Goelles and BØggild, 2017). The LAPs from meltout and the atmospheric deposition enriched in the surface. Data on LAP concentrations in glacier ice were obtained from the ice pit at the site of the AWS in August 2016 (Li et al., 2019b); the concentration in the surface was the average concentration in the top 5 cm of the ice pit, and the LAP concentration in the englacial ice was the minimum concentration of the ice pit.

3.3 Surface energy and mass balance model

To assess glacier melting caused by LAPs, a surface energy and mass balance model was used, which can be expressed as follows:

$$B = \int \left(\frac{Q_M}{L_m} + \frac{LE}{L_v} + C_{en} + P_{snow}\right) dt \, , \quad (1)$$

where B is the net mass balance (mm w.e.), Q_M is melt energy, LE is turbulent latent heat flux; L_m is the latent heat of ice melting (3.34×10^5 J kg^{-1}); L_v is the heat of evaporation/sublimation (2.51×10^6/2.85×10^6 J kg^{-1}), which is determined by glacier surface temperature; C_{en} is refreezing of meltwater; P_{snow} is accumulation of solid precipitation; and Q_M is calculated from the surface energy balance model equation:

$$Q_M = S\downarrow(1-\alpha) + L^{\downarrow} + L^{\uparrow} + H + LE + Q_G \, , \quad (2)$$

where $S^{\downarrow}$ is the incoming solar radiation; α is the surface albedo; $L^{\downarrow}$ and $L^{\uparrow}$ are the incoming and outgoing longwave radiation, respectively; the sensible (H) and latent heat (LE) fluxes are calculated using the aerodynamic method (Chen et al., 2017); and Q_G is the subsurface heat flux, which is estimated from the temperature–depth profile

https://doi.org/10.5194/tc-2022-179
Preprint. Discussion started: 30 September 2022

(Sun et al., 2014). On the right-hand side of Eq. (2), all energy components are defined as positive when they are directed toward the surface and negative when they are directed away from the surface.

The surface energy and mass balance model were driven using surface meteorological measurements with 30-min temporal resolution. The surface energy and mass components were simulated by the model at intervals of 100 m in elevation, and the lapse rates of temperature and precipitation were determined using measurements obtained by two AWSs (Chen et al., 2017). All parameters adopted in model are shown in Table 1.

3.4 Albedo model

To quantify the effect of BC on glacier melting, an albedo model incorporating LAPs was employed (Gardner and Sharp, 2010). The model approximates the physical-based parameterized snow albedo as the sum of pure snow/ice albedo (α_{SSA}) and the change caused by LAPs ($\mathrm{d}\alpha_c$) and solar altitude angle ($\mathrm{d}\alpha_{\theta z}$):

$$\alpha = \alpha_{SSA} + \mathrm{d}\alpha_c + \mathrm{d}\alpha_{\theta z}. \tag{3}$$

The value of α_{SSA} is calculated as a function of the specific surface area (SSA):

$$\alpha_{\mathrm{SSA}} = 1.48 - \mathrm{SSA}^{-0.07}. \tag{4}$$

In this albedo model, BC is assumed to be externally mixed with snow grains, and therefore the change of albedo can be expressed as follows:

$$\mathrm{D}\alpha_C = \max\left(0.04 - \alpha_{\mathrm{SSA}}, \frac{-C^{0.55}}{0.16+0.6\mathrm{SSA}^{0.5}+1.8C^{0.6}\mathrm{SSA}^{-0.25}}\right), \tag{5}$$

where C is the concentration of LAPs (mg kg^{-1}). The MD concentration was converted to an optically equivalent concentration of BC using a mass absorption coefficient (MAC). Values of MACs for BC and MD were chosen as 4.28 and 0.011 m^2 g^{-1}, as suggested by Li et al. 2021 based on measurements on the LHG glacier.

Here, $\mathrm{d}\alpha_{\theta z}$ is calculated as a function of solar altitude angle (θ_z) and α_{SSA}:

$$\mathrm{d}\alpha_{\theta_z} = 0.53\alpha_{SSA}(1-(\alpha_{SSA}+d\alpha_c))(1-\cos\theta_z)^{1.2}. \tag{6}$$

In calculation of albedo, SSA is a key parameter that is defined as the sum of the areas per unit mass. In this paper, SSA was calculated separately depending on dry and wet snow metamorphism (Roy et al., 2013; Gabbi et al., 2015). In the case of dry snow

https://doi.org/10.5194/tc-2022-179
Preprint. Discussion started: 30 September 2022

conditions, the variation of SSA was calculated according to Taillandier et al. 2007 as a logarithmic function of snow age and snow temperature (T_{snow}):

$$\mathrm{SSA(t)} = [0.629 \cdot \mathrm{SSA}_{\mathrm{initial}} - 15.0 \cdot (T_{snow} - 11.2)] - [0.076 \cdot \mathrm{SSA}_{\mathrm{initial}} - 1.76 \cdot (T_{snow} - 2.96)] \cdot \ln\left\{t + e^{\frac{-0.371 \cdot \mathrm{SSA}_{\mathrm{inital}} - 15.0 \cdot (T_{snow} - 11.2)}{0.076 \cdot \mathrm{SSA}_{\mathrm{inital}} - 1.76 \cdot (T_{snow} - 2.96)}}\right\}. \quad (7)$$

In the case of wet snow conditions, we referred to the method of Gabbi et al. 2015. The growth of the optical radius of snow (ΔR_{opt}) can be expressed as follows:

$$\Delta R_{opt} = \frac{C_1 + C_2 \cdot \theta^3}{R_{opt}^2 \cdot 4\pi}, \quad (8)$$

where C_1 and C_2 are empirical coefficients with values of 1.1×10^{-3} and 3.7×10^{-5} mm d^{-1}, respectively, and θ is the liquid water content expressed as a mass percentage. Change of the optical radius of snow is greatly influenced by θ, and SSA decreases rapidly when θ increases. The equivalent optical radius (R_{opt}) is derived from SSA and ice density (ρ_{ice}):

$$R_{opt} = \frac{3}{\rho_{ice} \cdot SSA}. \quad (S9)$$

When a glacier starts melting, the SSA model shifts from dry snow conditions to wet snow conditions. At this moment, the initial SSA is known. Then, Eq. (8) is applied in which R_{opt} is computed using the initial value of SSA according to Eq. (9); thus, a new SSA value is generated. We set a fresh snow SSA value of 1000 cm^2 g^{-1} to match the measured highest albedo of fresh snow, and a minimal SSA value of 80 cm^2 g^{-1} (Taillandier et al., 2007; Gabbi et al., 2015). We used a value of SSA of 1.6 cm^2 g^{-1} for ice (Goelles and BØggild, 2017).

Table 1. Initial conditions and parameters involved in the model.

Parameters	Value	Source
Initial BC concentration of ice surface (ng g^{-1})	1688	Li et al. 2019b
Initial MD concentration of ice surface (μg g^{-1})	1130	Li et al. 2019b
BC concentration of englacial ice (ng g^{-1})	47.5	Li et al. 2019b
MD concentration of englacial ice (ng g^{-1})	15.3	Li et al. 2019b
BC concentration of precipitation (ng g^{-1})	21.8	Li et al. 2019c
Removal efficiency of BC	0.2	Doherty et al. 2013
Density of snow (g cm^{-3})	0.3	
Density of ice (g cm^{-3})	0.9	
Lapse rate of temperature (°C / 100 m)	-0.052	Measurements
Lapse rate of precipitation (% / 100 m)	4.5	Measurements
Roughness length for ice (mm)	1.6	Sun et al. 2014

https://doi.org/10.5194/tc-2022-179
Preprint. Discussion started: 30 September 2022

Roughness length for firn	5.3	Sun et al. 2014
Refreezing rate of melt water	0.26	Optimized value

4 Results

4.1 Calibration and Validation

The surface energy and mass balance model used contained a parameterization of albedo with inputs of LAPs and specific surface area for snow and ice. All parameters used in the model are listed in Table 1. We assumed that the refreezing of meltwater occurred in the snow layer, which was tuned to the accumulated mass balance during May 1 to August 31. The procedure was repeated at the site of the AWS until the root mean square error (*RMSE*) between the simulated and measured mass balance was smallest. Finally, an optimized refreezing rate was obtained with a value of 0.26 (Table 1). The simulated accumulated mass balance was highly consistent with the measured value with the smallest *RMSE* of 36 mm w.e. and less than 10% of the mass balance. The modeled albedo was in reasonable agreement with the measured albedo with R^2 and *RMSE* values of 0.67 (n = 365, p < 0.001) and 0.01, respectively (Fig. 3a). Using the calibrated refreezing rate of meltwater, the surface energy and the mass balance were simulated at intervals of 100 m in elevation.

To further validate the model performance, the differences between the simulated and measured variations of snow height at 5050 m a.s.l. and annual mass balance of each elevation belt were compared (Fig. 4). Snow height at 5050 m a.s.l. was measured using a sonic range sensor (Chen et al., 2018). The measured snow height was 197 mm higher on average than the simulated snow height, which is equivalent to a mass balance of 59 mm w.e. for snow density of 0.3 g cm^{-3}. The discrepancy derived mainly from the simulation in the non-melt season attributable to drifting snow and errors in precipitation measurements. The simulated annual mass balance was also in reasonable agreement with that measured at each elevation belt, with a value of *RMSE* of 121 mm w.e. and less than 10% of the measured average mass balance (−1218 mm w.e.). This simulation was referred to as “Stand_Run.”

https://doi.org/10.5194/tc-2022-179
Preprint. Discussion started: 30 September 2022

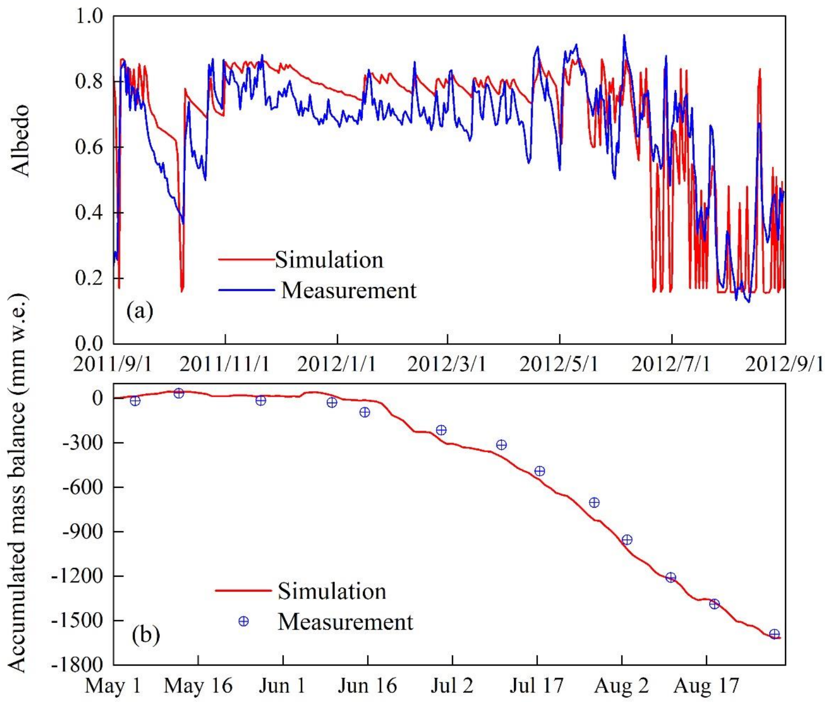

Fig. 3 Comparisons between simulation and measurement of (a) albedo and (b) accumulated mass balance at site of AWS.

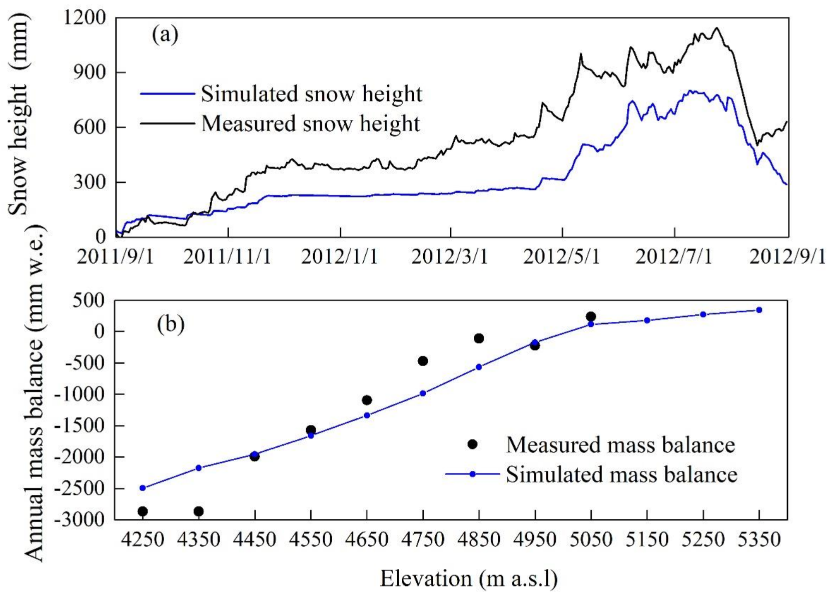

https://doi.org/10.5194/tc-2022-179
Preprint. Discussion started: 30 September 2022

Fig. 4 Comparisons between simulation and measurement of (a) albedo and (b) accumulated mass balance at the site of the AWS.

4.2 Variation in surface BC and MD concentrations

As shown in Fig. 5, LAPs concentration was correlated negatively with surface snow because the surface with high concentration was covered by fresh snow. The concentration of LAPs remained low during the cold season (September–April), whereas it increased substantially during the melt season (May–August) owing to strong melting. The average surface concentration of BC ranged from 815 ng g^{-1} at the lowest elevation to 166 ng g^{-1} at highest elevation during the cold season, whereas it ranged from 2091 to 477 ng g^{-1} at corresponding elevations during the warm season. The average surface concentration of MD ranged from 329 µg g^{-1} at the lowest elevation to 166 µg g^{-1} at the highest elevation during the cold season, whereas it ranged from 1068 to 266 µg g^{-1} at corresponding elevations during the warm season. Our results are in the same order with Zhang et al. 2017b, which reported that BC concentrations in surface snow are in the range of 193–11040 ng g^{-1} during four expeditions on the LHG glacier, but they also showed extremely high concentration in transient and single-point snow sample.

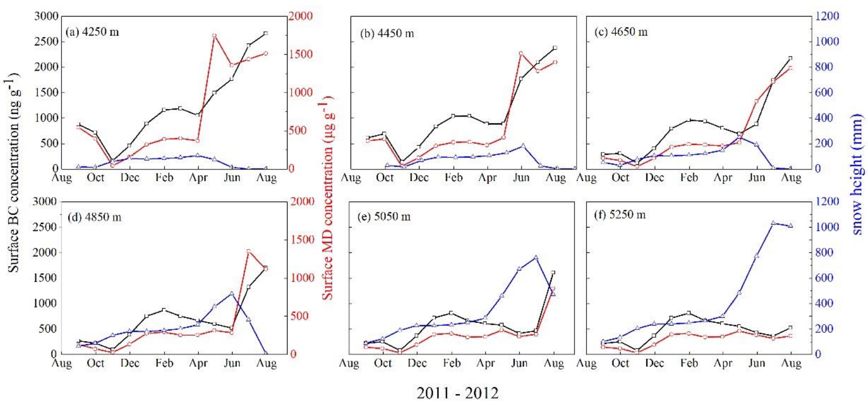

Fig. 5 Monthly snow height (blue line), BC concentration (black line), and MD concentration (red line) at elevation intervals of 200 m in the LHG glacier

https://doi.org/10.5194/tc-2022-179
Preprint. Discussion started: 30 September 2022

4.3 LAPs effect on surface albedo

To explore the effect of LAPs on glacier melting, we set a series of experiments for removal of different types of LAPs (Table 2). The effect of BC and MD on the surface albedo was greater during the melt season than during the cold season, and it decreased with increasing elevation (Fig. 6a, b). Annually, the effect of BC was comparable to that of MD, whereas the effect of BC was smaller than that of MD during the melt season, and this phenomenon was more obvious in July and August with the strongest melting (Fig. 6e, f). The sum of the effects of the separate removal of BC and MD on albedo was much less than that of the removal of both BC and MD in the ablation zone, and the difference was more obvious with intensification of melting and less obvious with increasing elevation. The average albedo during the entire year and the melt season was 0.76 and 0.69, respectively, in Stand_Run. The effect of BC and MD on glacier-wide albedo was consistent with a value of 0.02 during the entire year and values of 0.03 and 0.04 for BC and MD, respectively, during the melt season (Table 2). When BC and MD were both removed, the increment of albedo was 0.08 during the entire year and 0.13 during the melt season.

https://doi.org/10.5194/tc-2022-179
Preprint. Discussion started: 30 September 2022

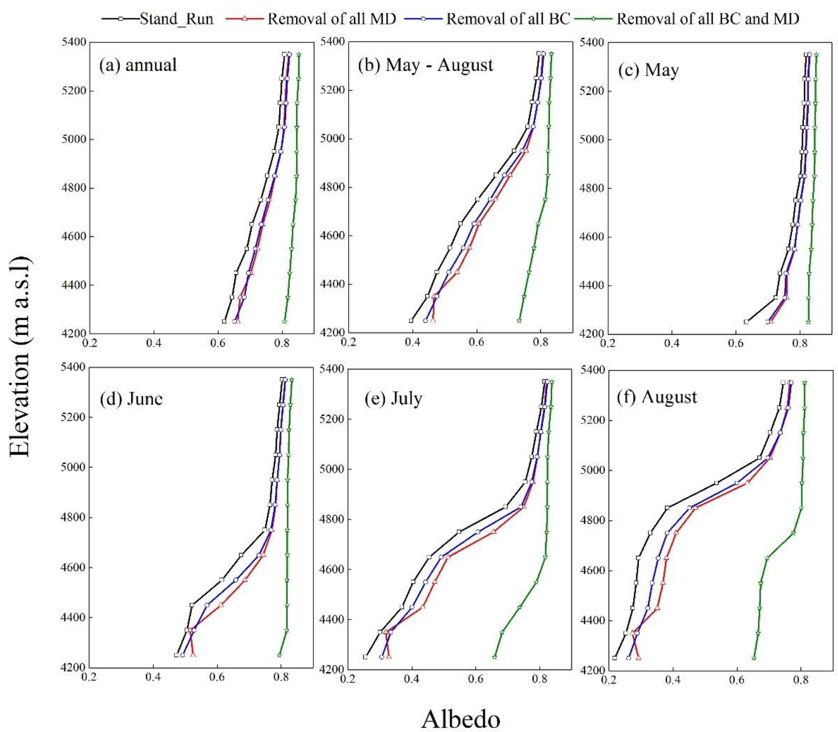

Fig. 6 Average albedo at intervals of 100 m in elevation under scenarios of Stand_Run (black line), removal of all MD (red line), removal of all BC (blue line), and removal of all BC and MD together during (a) the entire year, (b) May–August, (c) May, (d) June, (e) July, and (f) August.

Table 2 Glacier-wide average albedo and accumulated melting under scenarios of removing Laps, values in parentheses refer to ratio of LAPs effect on melting

	Albedo		Melting (mm w.e.)	
	Annual	Melt season	Annual	Melt season
Stand_Run	0.76	0.69	960	934
Removal of all MD	0.78	0.73	820 (14.6%)	798 (14.6%)
Removal of all BC	0.78	0.72	834 (13.1%)	851 (12.3%)
Removal of BC and MD	0.84	0.82	410 (57.3%)	399 (57.3%)

4.4 LAPs effect on glacier melting

During the cold season, the effect of BC on glacier mass balance was greater than that

https://doi.org/10.5194/tc-2022-179
Preprint. Discussion started: 30 September 2022

of MD; however, the effect became very weak at elevations above ~5000 m a.s.l. (Fig. 7a) because of minimal melting at such elevations. The effect of BC on glacier mass balance was less than that of MD during the melt season (Fig. 7b). The annual glacier-wide mass balance was −361 mm w.e. in Stand_Run, whereas it was −238 mm w.e. when all MD was removed and −254 mm w.e. when all BC was removed.

Alone, BC contributed to 13.1% of glacier melting during the full year and 12.3% during the melt season, whereas MD alone contributed to 14.6% of glacier melting during the full year and melt season. Glacier melting was aggravated by 57.3% under the combined effect of BC and MD. The contribution of BC to melting on the LHG glacier was less than that reported on the Mera glacier (16%, Ginot et al., 2014) and on the Claridenfirn glacier (15%–19%, Gabbi et al., 2015). However, the combined contribution of BC and MD to melting was much greater on the LHG glacier than on the Mera glacier (26%). This is because there is an approximate logarithmic relationship between the concentration of LAPs and albedo reduction, i.e., albedo declines rapidly with increase of LAPs in the case of low concentration of LAPs, whereas it declines slowly with increase of LAPs in the case of high concentration of LAPs.

The concentrations of BC and MD are very high in the surface ice on the LHG glacier; hence, considering either BC or MD alone has a limited effect on the surface albedo. Other earlier studies calculated the reduction in albedo of pure snow or ice attributable to BC without contamination by MD, and assessed the impact on glacier melting caused by albedo reduction using a simple melt model (Li et al., 2016; Li et al., 2019b; Li et al., 2019a; Zhang et al., 2017a). Generally, the calculated albedo reduction was higher for pure snow or ice than for contaminated snow or ice when the BC concentration remained constant. For example, Li et al. 2016 reported contributions to melting by BC alone (37%) and MD alone (32%) that were much greater than our results for the LHG glacier, whereas the combined contribution of BC and MD (61%) was similar to our findings. However, our findings are of greater practical importance regarding implications for policies intended to abate contamination of glaciers by LAPs.

https://doi.org/10.5194/tc-2022-179
Preprint. Discussion started: 30 September 2022

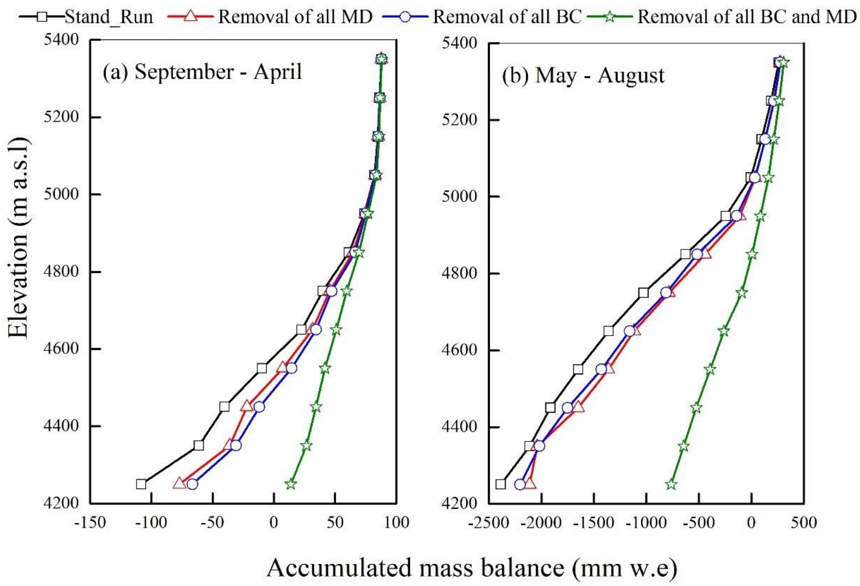

Fig. 7 Accumulated mass balance at intervals of 100 m in elevation during (a) September–April and (b) May–August under the scenarios of Stand_Run (black line), removal of all MD (red line), removal of all BC (blue line), and removal of all BC and MD.

5 Discussion

5.1 Different mechanisms of BC impact on glacier melting

In this study, we identified three mechanisms via which BC affects glacier melting (Fig. 8). The BC from meltout ice and atmospheric wet deposition had little influence on the glacier mass balance, whereas the BC from atmospheric dry deposition caused 68 mm w.e. of glacier-wide mass balance change (Table 3). Total BC from atmospheric deposition caused 9.1% of glacier melt change during the full year and 8.8% during the melt season, of which dry deposited BC caused 8.3% of glacier melt change during the full year and 7.9% during the melt season. Gabbi et al. 2015 reported amplification of annual melt rates by 10% (12%) at the upper (lower) stake on the Claridenfirn glacier in the Swiss Alps attributable to atmospheric deposited BC, which is similar to our findings and demonstrates the universal effect of the emission of BC associated with human activities on glacier melting.

https://doi.org/10.5194/tc-2022-179
Preprint. Discussion started: 30 September 2022

The effect of meltout BC on glacier melting was negligible with a value of 1.9% during the full year and 2.2% during the melt season. This finding is different from that reported by Goelles et al. 2017 who found a strong contribution of meltout BC to glacier melting. The concentration of LAPs on surface ice can be very high and inhomogeneous (Li et al., 2016; Zhang et al., 2017b). The processes of enrichment and removal of LAPs on the ice surface are complex and remain unclear. For example, LAPs could be washed away by surface flowing water with low concentration in steep areas, or enriched in a cryoconite hole in a flat area. The removal efficiency of LAPs in surface ice might be related to factors such as initial concentration, slope gradient, and flow magnitude. However, owing to lack of available related measurements, it remains difficult to establish a reasonable physical model. Using a constant removal efficiency for LAPs in surface ice could elevate the surface concentration to an unrealistically high value. To avoid unrealistic enhancement of LAPs concentration in a year, we assumed that all LAPs were enriched and distributed evenly throughout the upper 20 cm of surface ice rather than the upper 5 or 2 cm. This approach maintained the LAPs concentration within a reasonable range while weakening the effects of deposited and meltout BC on glacier melting.

https://doi.org/10.5194/tc-2022-179
Preprint. Discussion started: 30 September 2022

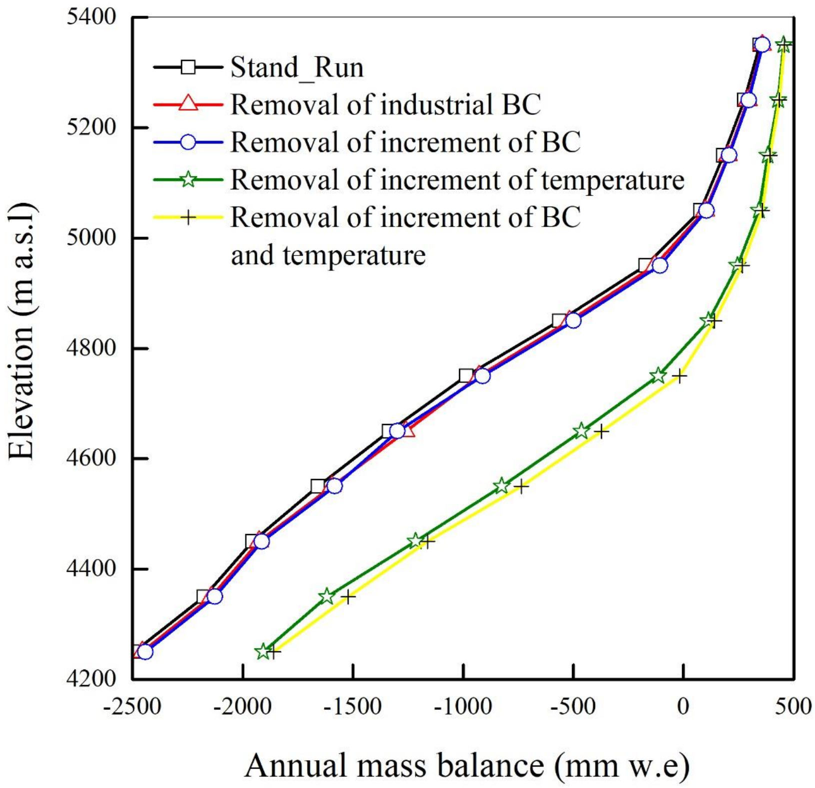

375

376 **Fig. 8** Annual mass balance at intervals of 100 m in elevation under scenarios of

377 Stand_Run (black line), removal of all BC from fossil fuel (red line), removal of

378 increment of BC deposition since the 1980s (blue line), reduction of temperature by

379 1.5 °C (green line), and both removal of increment of BC deposition and reduction of

380 temperature by 1.5 °C (yellow line).

381

382 **Table 3.** Glacier-wide average albedo and accumulated melting under scenarios of

383 removing LAPs.

	Melting (mm w.e.)		Mass balance (mm w.e.)	
	Annual	Melt season	Annual	Melt season
Stand_Run	960	934	-361	-422
Removal of BC from atmosphere	873 (9.1%)	852 (8.8%)	-284	-359

https://doi.org/10.5194/tc-2022-179
Preprint. Discussion started: 30 September 2022

Removal of BC from atmospheric dry deposition	880 (8.3%)	860 (7.9%)	-293	-368
Removal of BC from atmospheric wet deposition	947 (1.4%)	922 (1.3%)	-354	-413
Removal of BC from Meltout ice	942 (1.9%)	913 (2.2%)	-348	-416
Removal of BC from industrial emission	911 (5.1%)	885 (5.2)	-322	-379
Removal of BC increment since 1980s	896 (6.7%)	875 (6.3%)	-296	-361
Temperature drops 1.5 °C	462 (51.9%)	455 (51.3%)	87	11
Removal BC increment and temperature drops 1.5 1.5 °C	424 (55.8%)	417 (56.6%)	119	42

5.2 Accelerated glacier melting caused by increments in BC emissions and air temperature

The temperature on the LHG glacier has increased by approximately 1.5 °C since the 1950s (Chen et al., 2019; Qin et al., 2015). Records of BC in an ice core from the Eastern Pamirs show that the average concentration of BC after the 1990s was 4.6 times higher than that during the early Industrial Revolution (Wang et al., 2015). We modeled the surface energy and mass balance under a scenario of reducing the atmospheric deposited BC by 4.6 times (Table 3). The modeled annual glacier-wide mass balance was less negative by 65 mm w.e. than the mass balance in Stand_Run, i.e., the increased emission of BC by human activities accelerated current glacier melting by 6.3%. However, the glacier-wide mass balance would be positive with a value of 87 mm w.e. under a scenario in which the temperature was reduced by 1.5 °C, i.e., the increase in temperature contributed to 51.9% of current glacier melting. Glacier melting would reduce by 55.8% under a scenario without increments in BC and warming.

From the above analysis, we conclude that warming has been the dominant factor in the current accelerated melting of the LHG glacier, while the increment of BC emissions since the Industrial Revolution has further aggravated glacier melting. There are no studies that directly focus on the effect of the BC increment since the early Industrial Revolution on glacier melting. Gabbi et al. 2015 reported an average

https://doi.org/10.5194/tc-2022-179
Preprint. Discussion started: 30 September 2022

contribution of 10% of total atmospheric BC on glacier melting during 1914–2014. Moreover, BC records from ice cores show that the peak of BC emissions in Europe and North America occurred during 1900–1950 (Sigl et al., 2013; Thevenon et al., 2009; Jenk et al., 2009), and that the BC concentration in recent decades has been no larger than 3 times that during the early Industrial Revolution. Thus, we could infer that the effect of increased BC on current glacier melting is less than 10%.

Painter et al. 2013 suggested that the end of the Little Ice Age in the European Alps was forced by emission of industrial BC; however, Sigl et al. 2018 refuted that supposition, believing instead that the 19th century glacier retreat in the Alps preceded the emergence of industrial BC deposition on high-alpine glaciers. Our results cannot substantiate the effect of industrial BC on glacier melting during the Little Ice Age. However, this study underestimated the effect of deposited BC on glacier ice melting. Moreover, most of the BC emitted in the past has enriched surface concentrations over a long period, and the concentration of BC in surface ice might not be so high if there had not been continuous emission of BC since the Industrial Revolution. To accurately model the effect of BC emitted by human activities on glacier melting, measurements of BC enrichment in and removal from surface ice are essential.

5.3 Significance of glacier melting mitigation

This study provided a conservative estimation of effect of emitted BC by current human activities on glacier melting. It was concluded that the glacier melting would reduce at least by 6.3% if the BC emission was brought back to pre-industrial levels. Moreover, the existed BC in glacier surface might be moved down to downstream of by glacier movement or washed away by melt water, if the BC emission reduction continued year by year. Then the mitigation of glacier melting would be larger than 6.3%, but probably not larger than 13.1%.

4. Conclusion

In this study we developed an atmospheric deposition and spatiotemporal distribution model of LAPs (BC and MD) on glacier surface, and coupled the model into a surface energy and mass balance model including a parameterization for albedo with

https://doi.org/10.5194/tc-2022-179
Preprint. Discussion started: 30 September 2022

parameters of concentration of LAPs and SSA of snow and ice. Using the combined model forced with measured surface meteorological variables, we assessed LAPs, especially atmospheric deposited BC effects on surface energy and mass balance during 2011 – 2012 on the LHG glacier in the western Qilian Mountains. The model was calibrated by the measured surface albedo and mass balance at 4550 m a.s.l. The model performance was validated by measured annual mass balance extended to the entire glacier at intervals of 100 m in elevation.

The average surface concentration of BC ranged from 2091 ng g-1 at the lowest site in elevation to 477 ng g-1 at the highest site during warm season (May – August), which caused reduction of 0.03 in glacier-wide albedo and increase of 12.3% in glacier melting. The average surface concentration of MD ranged from 1068 μg g-1 to 266 μg g-1 during warm season, which caused reduction of 0.04 in glacier-wide albedo and increase of 14.6% in glacier melting. Nevertheless, the combined effect of BC and MD was 0.13 (0.08) on glacier-wide albedo and 57.3% (57.3%) on glacier melting during the melt season (full year).

This study emphasized the BC effect on glacier melting, because it main came from human activities emission. We have assessed BC from atmosphere effect on glacier melting. The total effect of atmospheric deposited BC was 9.1% on annual glacier-wide melting, of which BC from atmospheric dry deposition had an effect of 8.3% on melting. The deposited BC from fossil fuel combustion caused 5.1% of glacier melting.

The temperature and BC emission by human activities all have dramatically increased since the 1950s. We assessed the increased temperature and BC emission respective contribution to current accelerated glacier melting. The temperature during recent two decades increased by 1.5 °C compared to that during 1950s, which caused 51.9% of annual glacier-wide melting. Meanwhile, the BC emission increased by 4.6 times compared to the early Industrial Evolution, which caused 6.7% of annual glacier-wide melting.

The enrichment and removal of LAPs on surface ice are really complicated, method in handling them used in the research underestimated deposited BC effect on glacier

https://doi.org/10.5194/tc-2022-179
Preprint. Discussion started: 30 September 2022

melting. However, the ice melting plays a very important role in glacier melting, while it is still unknown about its approach and key parameters of concentration change of LAIs on it. To illuminate it with accuracy and clarity, substantial observations of variation of LAIs on ice surface are really needed.

Data Availability: The datasets generated during and/or analysed during the current study are available via linking to chenjizu@lzb.ac.cn

Author contribution: All authors contributed to the study conception and design. Jizu Chen and Shichang Kang designed the experiments and Wentao Du carried them out. Material preparation and data collection were performed by Xiang Qin, Yang Li and Yushuo Liu. Data analysis and software were performed by Lihui Luo, Weijun Sun and Youyan Jiang.

Competing Interests: The authors have no relevant financial or non-financial interests to disclose.

Acknowledgments:

This study was supported by the Second Tibetan Plateau Scientific Expedition and Research Program (2019QZKK0605), the National Natural Science Foundation of China (42101139, 42071018, 41971073), the State Key Laborartory of Cryospheric Science (SKLCS-ZZ-2022), and CAS "Light of West China" Program.

References:

Azam, M. F., Wagnon, P., Berthier, E., Vincent, C., Fujita, K., and Kargel, J. S.: Review of the status and mass changes of Himalayan-Karakoram glaciers, Journal of Glaciology, 64, 61-74, 10.1017/jog.2017.86, 2018.

Bond, T. C., Doherty, S. J., Fahey, D. W., Forster, P. M., Berntsen, T., DeAngelo, B. J., Flanner, M. G., Ghan, S., Kärcher, B., Koch, D., Kinne, S., Kondo, Y., Quinn, P. K., Sarofim, M. C., Schultz, M. G., Schulz, M., Venkataraman, C., Zhang, H., Zhang, S., Bellouin, N., Guttikunda, S. K., Hopke, P. K., Jacobson, M. Z., Kaiser, J. W., Klimont, Z., Lohmann, U., Schwarz, J. P., Shindell, D., Storelvmo, T., Warren, S. G., and Zender, C. S.: Bounding the role of black carbon in the climate system: A scientific assessment, Journal of Geophysical Research: Atmospheres, 118, 5380-5552, 10.1002/jgrd.50171, 2013.

Brun, F., Berthier, E., Wagnon, P., Kaab, A., and Treichler, D.: A spatially resolved estimate of High Mountain Asia glacier mass balances, 2000-2016, Nature Geoscience, 10, 668-673, 10.1038/NGEO2999, 2017.

Chen, J., Kang, S., Qin, X., Du, W., Sun, W., and Liu, Y.: The mass-balance characteristics and sensitivities to climate variables of Laohugou Glacier No. 12, western Qilian Mountains, China, Science in cold and arid regions, 9, 543-553, 10.3724/SP.J.1226.2017.00543, 2017.

https://doi.org/10.5194/tc-2022-179
Preprint. Discussion started: 30 September 2022

Chen, J., Qin, X., Kang, S., Du, W., Sun, W., and Liu, Y.: Effects of clouds on surface melting of Laohugou glacier No. 12, western Qilian Mountains, China, Journal of Glaciology, 1-11, 10.1017/jog.2017.82, 2018.

Chen, J., Qin, X., Kang, S., Du, W., Sun, W., and Liu, Y.: Potential Effect of Black Carbon on Glacier Mass Balance during the Past 55 Years of Laohugou Glacier No. 12, Western Qilian Mountains, Journal of Earth Science, 31, 410-418, 10.1007/s12583-019-1238-5, 2019.

Conway, H., Gades, A., and Raymond, C. F.: Albedo of dirty snow during conditions of melt, Water Resources Research, 32, 1713-1718, 10.1029/96wr00712, 1996.

Doherty, S. J., Grenfell, T. C., Forsström, S., Hegg, D. L., Brandt, R. E., and Warren, S. G.: Observed vertical redistribution of black carbon and other insoluble light-absorbing particles in melting snow, Journal of Geophysical Research: Atmospheres, 118, 5553-5569, 10.1002/jgrd.50235, 2013.

Dong, Z., Qin, D., Kang, S., Ren, J., Chen, J., Cui, X., Du, Z., and Qin, X.: Physicochemical characteristics and sources of atmospheric dust deposition in snow packs on the glaciers of western Qilian Mountains, China, Tellus B: Chemical and Physical Meteorology, 66, 20956, 10.3402/tellusb.v66.20956, 2014.

Farinotti, D., Huss, M., Fürst, J. J., Landmann, J., Machguth, H., Maussion, F., and Pandit, A.: A consensus estimate for the ice thickness distribution of all glaciers on Earth, Nature Geoscience, 12, 168-173, 10.1038/s41561-019-0300-3, 2019.

Flanner, M. G., Zender, C. S., Randerson, J. T., and Rasch, P. J.: Present-day climate forcing and response from black carbon in snow, Journal of Geophysical Research, 112, 10.1029/2006jd008003, 2007.

Gabbi, J., Huss, M., Bauder, A., Cao, F., and Schwikowski, M.: The impact of Saharan dust and black carbon on albedo and long-term glacier mass balance, The Cryosphere Discussions, 9, 1133-1175, 10.5194/tcd-9-1133-2015, 2015.

Gardner, A. S. and Sharp, M. J.: A review of snow and ice albedo and the development of a new physically based broadband albedo parameterization, Journal of Geophysical Research, 115, 10.1029/2009jf001444, 2010.

Ginot, P., Dumont, M., Lim, S., Patris, N., Taupin, J. D., Wagnon, P., Gilbert, A., Arnaud, Y., Marinoni, A., Bonasoni, P., and Laj, P.: A 10 year record of black carbon and dust from a Mera Peak ice core (Nepal): variability and potential impact on melting of Himalayan glaciers, The Cryosphere, 8, 1479-1496, 10.5194/tc-8-1479-2014, 2014.

Goelles, T. and BØGgild, C. E.: Albedo reduction of ice caused by dust and black carbon accumulation: a model applied to the K-transect, West Greenland, Journal of Glaciology, 63, 1063-1076, 10.1017/jog.2017.74, 2017.

Han, Y. M., Wei, C., Bandowe, B. A., Wilcke, W., Cao, J. J., Xu, B. Q., Gao, S. P., Tie, X. X., Li, G. H., Jin, Z. D., and An, Z. S.: Elemental carbon and polycyclic aromatic compounds in a 150-year sediment core from Lake Qinghai, Tibetan Plateau, China: influence of regional and local sources and transport pathways, Environ Sci Technol, 49, 4176-4183, 10.1021/es504568m, 2015.

Hock, R.: Temperature index melt modelling in mountain areas, Journal of Hydrology, 282, 104-115, 10.1016/s0022-1694(03)00257-9, 2003.

Hugonnet, R., McNabb, R., Berthier, E., Menounos, B., Nuth, C., Girod, L., Farinotti, D., Huss, M., Dussaillant, I., Brun, F., and Kaab, A.: Accelerated global glacier mass loss in the early twenty-first century, Nature, 592, 726-731, 10.1038/s41586-021-03436-z, 2021.

Jenk, T. M., Szidat, S., Bolius, D., Sigl, M., Gäggeler, H. W., Wacker, L., Ruff, M., Barbante, C., Boutron, C. F., and Schwikowski, M.: A novel radiocarbon dating technique applied to an ice core from the Alps indicating late Pleistocene ages, Journal of Geophysical Research, 114, 10.1029/2009jd011860, 2009.

Kang, S., Zhang, Y., Qian, Y., and Wang, H.: A review of black carbon in snow and ice and its impact on the cryosphere, Earth-Science Reviews, 210, 103346, 10.1016/j.earscirev.2020.103346, 2020.

Kaspari, S., Mckenzie Skiles, S., Delaney, I., and Painter, T. H.: Accelerated glacier melt on snow dome, Mounta Olympus, Washingdon, USA, due to deposition of black carbon and mineral dust from wildfire, Journal of Geophysical Research Atmosphere, 7, 2793-2807, 10.1002/2014JD022676, 2015.

Li, X., Kang, S., Sprenger, M., Zhang, Y., He, X., Zhang, G., Tripathee, L., Li, C., and Cao, J.: Black carbon and mineral dust on two glaciers on the central Tibetan Plateau: sources and implications, Journal of Glaciology, 66, 248-258, 10.1017/jog.2019.100, 2019a.

Li, Y., Kang, S., Yan, F., Chen, J., Wang, K. U. N., Paudyal, R., Liu, J., Qin, X., and SillanpÄÄ, M.: Cryoconite on a glacier on the north-eastern Tibetan plateau: light-absorbing impurities, albedo and enhanced melting, Journal of Glaciology, 65, 633-644, 10.1017/jog.2019.41, 2019b.

Li, Y., Kang, S., Chen, J., Hu, Z., Wang, K., Paudyal, R., Liu, J., Wang, X., Qin, X., and Sillanpaa, M.: Black carbon in a glacier and snow cover on the northeastern Tibetan Plateau: Concentrations, radiative forcing and potential source from local topsoil, Sci Total Environ, 686, 1030-1038, 10.1016/j.scitotenv.2019.05.469, 2019c.

Li, Y., Chen, J., Kang, S., Li, C., Qu, B., Tripathee, L., Yan, F., Zhang, Y., Guo, J., Gul, C., and Qin, X.: Impacts of black carbon and mineral dust on radiative forcing and glacier melting during summer in the Qilian Mountains, northeastern Tibetan Plateau, The Cryosphere Discussions, 1-14, 10.5194/tc-2016-32, 2016.

Li, Y., Kang, S., Zhang, X., Chen, J., Schmale, J., Li, X., Zhang, Y., Niu, H., Li, Z., Qin, X., He, X., Yang, W., Zhang, G., Wang, S., Shao, L., and Tian, L.: Black carbon and dust in the Third Pole glaciers: Revaluated concentrations, mass absorption cross-sections and contributions to glacier ablation, Sci Total Environ, 789, 147746, 10.1016/j.scitotenv.2021.147746, 2021.

Li, Z., Li, H., and Chen, Y.: Mechanisms and simulation of accelerated shrinkage of continental glaciers: A case study of Urumqi Glacier No. 1 in eastern Tianshan, Central Asia, Journal of Earth Science, 22, 423-430, 10.1007/s12583-011-0194-5, 2011.

Liu, S., Zhang, Y., Zhang, Y., and Ding, Y.: Estimation of glacier runoff and future trends in the Yangtze River source region, China, Journal of Glaciology, 55, 353-362, 10.3189/002214309788608778, 2009.

Maurer, J. M., Schaefer, J. M., Rupper, S., and Corley, A.: Acceleration of ice loss across the Himalayas over the past 40 years, Science Advances, 5, eaav7266, DOI: 10.1126/sciadv.aav7266, 2019.

Ming, J., Cachier, H., Xiao, C., Qin, D., Kang, S., Hou, S., and Xu, j.: Black carbon record based on a shallow Himalayan ice core and its climatic implications, Atmospheric Chemistry and Physics, 8, 1343–1352, doi.org/10.5194/acp-8-1343-2008, 2008.

Painter, T. H., Flanner, M. G., Kaser, G., and Marzeion, B.: End of the Little Ice Age in the Alps forced by industrial black carbon, PNAS, 110, 15216–15221, 10.1073/pnas.1302570110, 2013.

Qian, Y., Yasunari, T. J., Doherty, S. J., Flanner, M. G., Lau, W. K. M., Ming, J., Wang, H., Wang, M., Warren, S. G., and Zhang, R.: Light-absorbing particles in snow and ice: Measurement and modeling of climatic and hydrological impact, Advances in Atmospheric Sciences, 32, 64-91, 10.1007/s00376-014-0010-0, 2015.

Qin, X., Chen, J., Wang, S., Sun, W., Du, W., and Liu, Y.: Reconstruction of surface air temperature in a glaciated region in the western Qilian Mountains, Tibetan Plateau, 1957–2013 and its variation characteristics, Quaternary International, 371, 22-30, 10.1016/j.quaint.2014.10.067, 2015.

Roy, A., Royer, A., Montpetit, B., Bartlett, P. A., and Langlois, A.: Snow specific surface area simulation

https://doi.org/10.5194/tc-2022-179
Preprint. Discussion started: 30 September 2022

using the one-layer snow model in the Canadian LAnd Surface Scheme (CLASS), The Cryosphere, 7, 961-975, 10.5194/tc-7-961-2013, 2013.

Sigl, M., Abram, N. J., Gabrieli, J., Jenk, T. M., Osmont, D., and Schwikowski, M.: 19th century glacier retreat in the Alps preceded the emergence of industrial black carbon deposition on high-alpine glaciers, The Cryosphere, 12, 3311-3331, 10.5194/tc-12-3311-2018, 2018.

Sigl, M., McConnell, J. R., Layman, L., Maselli, O., McGwire, K., Pasteris, D., Dahl-Jensen, D., Steffensen, J. P., Vinther, B., Edwards, R., Mulvaney, R., and Kipfstuhl, S.: A new bipolar ice core record of volcanism from WAIS Divide and NEEM and implications for climate forcing of the last 2000 years, Journal of Geophysical Research: Atmospheres, 118, 1151-1169, 10.1029/2012jd018603, 2013.

Sun, W., Qin, X., Du, W., Liu, W., Liu, Y., Zhang, T., Xu, Y., Zhao, Q., Wu, J., and Ren, J.: Ablation modeling and surface energy budget in the ablation zone of Laohugou glacier No. 12, western Qilian mountains, China, Annals of Glaciology, 55, 111-120, 10.3189/2014AoG66A902, 2014.

Taillandier, A.-S., Domine, F., Simpson, W. R., Sturm, M., and Douglas, T. A.: Rate of decrease of the specific surface area of dry snow: Isothermal and temperature gradient conditions, Journal of Geophysical Research, 112, 10.1029/2006jf000514, 2007.

Thevenon, F., Anselmetti, F. S., Bernasconi, S. M., and Schwikowski, M.: Mineral dust and elemental black carbon records from an Alpine ice core (Colle Gnifetti glacier) over the last millennium, Journal of Geophysical Research, 114, 10.1029/2008jd011490, 2009.

Wang, M., Xu, B., Kaspari, S. D., Gleixner, G., Schwab, V. F., Zhao, H., Wang, H., and Yao, P.: Century-long record of black carbon in an ice core from the Eastern Pamirs: Estimated contributions from biomass burning, Atmospheric Environment, 115, 79-88, 10.1016/j.atmosenv.2015.05.034, 2015.

Xu, B., Cao, J., Hansen, J., Yao, T., Joswia, D. R., Wang, N., Wu, G., Wang, M., Zhao, H., Yang, W., Liu, X., and He, J.: Black soot and the survival of Tibetan glaciers, Proc Natl Acad Sci U S A, 106, 22114-22118, 10.1073/pnas.0910444106, 2009.

Yao, T., Thompson, L., Yang, W., Yu, W., Gao, Y., Guo, X., Yang, X., Duan, K., Zhao, H., Xu, B., Pu, J., Lu, A., Xiang, Y., Kattel, D. B., and Joswiak, D.: Different glacier status with atmospheric circulations in Tibetan Plateau and surroundings, Nature Climate Change, 2, 663-667, 10.1038/nclimate1580, 2012.

Zhang, Y., Liu, S., and Ding, Y.: Observed degree-day factors and their spatial variation on glaciers in western China, Annals of Glaciology, 43, 301-306, 10.3189/172756406781811952, 2006.

Zhang, Y., Kang, S., Cong, Z., Schmale, J., Sprenger, M., Li, C., Yang, W., Gao, T., Sillanpää, M., Li, X., Liu, Y., Chen, P., and Zhang, X.: Light-absorbing impurities enhance glacier albedo reduction in the southeastern Tibetan plateau, Journal of Geophysical Research: Atmospheres, 122, 6915-6933, 10.1002/2016jd026397, 2017a.

Zhang, Y., Kang, S., Li, C., Gao, T., Cong, Z., Sprenger, M., Liu, Y., Li, X., Guo, J., Sillanpaa, M., Wang, K., Chen, J., Li, Y., and Sun, S.: Characteristics of black carbon in snow from Laohugou No. 12 glacier on the northern Tibetan Plateau, Sci Total Environ, 607-608, 1237-1249, 10.1016/j.scitotenv.2017.07.100, 2017b.

Zhang, Y., Kang, S., Sprenger, M., Cong, Z., Gao, T., Li, C., Tao, S., Li, X., Zhong, X., Xu, M., Meng, W., Neupane, B., Qin, X., and Sillanpää, M.: Black carbon and mineral dust in snow cover on the Tibetan Plateau, The Cryosphere, 12, 413-431, 10.5194/tc-12-413-2018, 2018.

Zhao, S., Ming, J., Xiao, C., Sun, W., and Qin, X.: A preliminary study on measurements of black carbon in the atmosphere of northwest Qilian Shan, Journal of Environmental Sciences, 24, 152-159, 10.1016/s1001-0742(11)60739-0, 2012.